

Fast optimization of parametrized quantum optical circuits

Filippo M. Miatto

*Institut Polytechnique de Paris and
Télécom Paris, LTCI, 19 Place Marguerite Perey 91120 Palaiseau*

Nicolás Quesada

Xanadu, Toronto, ON, M5G 2C8, Canada

(Dated: June 2, 2022)

Parametrized quantum optical circuits are a class of quantum circuits in which the carriers of quantum information are photons and the gates are optical transformations. Optimizing these circuits is challenging due to the infinite dimensionality of the photon number vector space that is associated to each optical mode. Truncating the space dimension is unavoidable, and it can lead to incorrect results if the gates populate photon number states beyond the cutoff. To tackle this issue, we present an algorithm that is orders of magnitude faster than the current state of the art, to recursively compute the exact matrix elements of Gaussian operators and their gradient with respect to a parametrization. These operators, when augmented with a non-Gaussian transformation such as the Kerr gate, achieve universal quantum computation. Our approach brings multiple advantages: first, by computing the matrix elements of Gaussian operators directly, we don't need to construct them by combining several other operators; second, we can use any variant of the gradient descent algorithm by plugging our gradients into an automatic differentiation framework such as TensorFlow or PyTorch. Our results will accelerate the research on quantum optical hardware, quantum machine learning, optical data processing, device discovery and device design.

I. INTRODUCTION

In recent years the success of machine learning (ML) in statistics, data science and artificial intelligence has sparked much interest in the field of quantum information and quantum computing. Nowadays, quantum machine learning is a term that encapsulates various techniques and ideas — including both optimization of quantum circuits via ML techniques [1, 2], as well as running subroutines of ML algorithms on quantum hardware [3, 4]. As a parallel thread, the quantum optics community has investigated how to compound quantum optical primitives to generate complex quantum states [5–9]. For this program to continue, it becomes necessary to develop new and efficient tools to perform fast simulation of quantum optical circuits.

Parametrized quantum circuits are information processing devices whose elements depend on one or more parameters, and therefore one can think of them as a particular class of neural networks [10–15]. Among parametrized quantum circuits, quantum optical circuits are those in which the carriers of quantum information are photons and the gates are optical transformations [6–8]. Working in the optical domain offers several advantages such as high processing speed, no demand for vacuum or cold temperatures and the potential to build compact devices via integrated optics [16–18].

A typical architecture of quantum optical circuits alternates between Gaussian transformations and non-linear ones such as the Kerr gate, which is necessary to achieve universality [19]. Although the evolution of Gaussian states under Gaussian transformations can be computed solely from their finite-dimensional symplectic matrix [20, 21], Kerr gates transform Gaussian states into non-

Gaussian ones and so they make it necessary to work in Fock space, which is infinite-dimensional and requires one to impose a cutoff.

Optimizing a parametrized quantum optical circuit is a challenging task, because one needs to simulate exactly the evolution of an input state as it propagates through the optical components, as well as the gradient of the output with respect to the circuit parameters. As each component can be represented in matrix form, the transformation of the initial state is a simple matrix multiplication and as such it is efficient. However, the difficult part is to generate the transformation matrix from the parameters of the gate: optical transformations (even the fundamental ones) are expressed as matrix exponentials of a linear combination of infinite-dimensional non-commuting operators [22]. Therefore (unless the exponent is diagonal) one cannot simply truncate the matrix at the exponent and subsequently compute the matrix exponential:

$$\text{trunc}(\exp(A)) \neq \exp(\text{trunc}(A)). \quad (1)$$

For some special transformations such as the displacement [23] and squeezing operator [24], exact formulas for their matrix elements are known. For some other transformations, such as two-mode squeezing and beamsplitters, one can resort to disentangling theorems which allow one to express the exponential in LDU form (i.e., as the product of a lower-triangular, a diagonal and an upper-triangular matrices), which can be safely truncated before multiplication, or alternatively allows the matrix elements to be expressed as polynomials of the parameters of the transformations [22, 25]. Bosonic representations of $SU(n)$ have also been studied in the mathematical physics literature [26]: in the quantum optical setting,

these are the matrix elements of a passive linear optical transformation corresponding to an interferometer. In the context of Franck-Condon transitions, the chemical-physics community [27–32] has studied the matrix elements of Gaussian transformations where the displacement, squeezing parameters and unitary matrices representing interferometers are real, corresponding to so-called point transformations where canonical positions and momenta of the harmonic oscillator do not mix [33–35]. For more general Gaussian transformations, until this work no exact method was known and typically one expressed them as a product of fundamental truncated gates, accepting that truncation errors could propagate.

Our method to perform the optimization of a parametrized quantum optical circuit has several advantages over previous techniques:

1. It generates recursively the matrix elements of general Gaussian transformations exactly up to the desired cutoff dimension without the need for decompositions. These results are derived in Sec. II for general Gaussian gates and applied to specific cases in Sec. III.
2. It constructs gradients exactly, without the need for computational graphs describing the functional dependencies between the variables. This is explained in Sec. IV.
3. It is numerically stable and orders of magnitude faster than previous methods. This is detailed in Sec. V where we report on several numerical experiments.

Our algorithms are part of the `fock_gradients` module of `The Walrus` [36] since version 0.12 released in Dec. 2019. Finally, note that in this work we construct recursively the matrix representation of a Gaussian operator. If instead one were interested in just a few specific matrix elements, one could map this to the calculation of loop hafnians [37, 38].

II. THE GENERATING FUNCTION METHOD

A. Notation and definitions

We summarize here our notational conventions, which are meant to simplify the presence of multiple indices in the multimode formulas, and the definition of our generating function.

We adopt the following short-hand notation:

$$\boldsymbol{\beta}^n \equiv \prod_{i=1}^{\ell} \beta_i^{n_i}, \quad (2)$$

$$\mathbf{n}! \equiv \prod_{i=1}^{\ell} n_i!. \quad (3)$$

We indicate tensor products of ℓ -mode coherent and Fock states as follows:

$$|\boldsymbol{\beta}\rangle = |\beta_1\rangle \otimes \dots \otimes |\beta_{\ell}\rangle, \quad (4)$$

$$|\mathbf{n}\rangle = |n_1\rangle \otimes \dots \otimes |n_{\ell}\rangle, \quad (5)$$

which we can use for instance to express a multimode coherent state:

$$|\boldsymbol{\beta}\rangle = e^{-\frac{1}{2}\|\boldsymbol{\beta}\|^2} \sum_{\mathbf{n}=0}^{\infty} \frac{\boldsymbol{\beta}^{\mathbf{n}}}{\sqrt{\mathbf{n}!}} |\mathbf{n}\rangle. \quad (6)$$

Note that tensor indices are numbered starting from 1 (as in Eq. (2)) while the indices themselves have values that begin from 0 (as in Eq. (6)). We also use interchangeably the following two notations for derivatives, depending on convenience and on the available space:

$$\frac{\partial^{\mathbf{k}}}{\partial \boldsymbol{\beta}^{\mathbf{k}}} = \partial_{\boldsymbol{\beta}}^{\mathbf{k}} \equiv \prod_i \frac{\partial^{k_i}}{\partial \beta_i^{k_i}}. \quad (7)$$

The key insight of the generating function method is that when we take the inner product of any operator \mathcal{G} (not just a Gaussian one) between two coherent states, we obtain a function of the coherent amplitudes that can be treated as a generating function for the matrix elements of \mathcal{G} :

$$\Gamma(\boldsymbol{\alpha}, \boldsymbol{\beta}) = e^{\frac{1}{2}(\|\boldsymbol{\alpha}\|^2 + \|\boldsymbol{\beta}\|^2)} \langle \boldsymbol{\alpha}^* | \mathcal{G} | \boldsymbol{\beta} \rangle \quad (8)$$

$$= \sum_{\mathbf{m}, \mathbf{n}=0}^{\infty} \frac{\boldsymbol{\alpha}^{\mathbf{m}} \boldsymbol{\beta}^{\mathbf{n}}}{\sqrt{\mathbf{m}! \mathbf{n}!}} \langle \mathbf{m} | \mathcal{G} | \mathbf{n} \rangle. \quad (9)$$

The matrix element $\langle \mathbf{m} | \mathcal{G} | \mathbf{n} \rangle$ is therefore contained in the coefficient of the factor $\boldsymbol{\alpha}^{\mathbf{m}} \boldsymbol{\beta}^{\mathbf{n}}$ in the Taylor series and we can isolate it by computing the derivatives of the appropriate order, at zero:

$$\mathcal{G}_{mn} \equiv \langle \mathbf{m} | \mathcal{G} | \mathbf{n} \rangle = \frac{\partial_{\boldsymbol{\alpha}}^{\mathbf{m}} \partial_{\boldsymbol{\beta}}^{\mathbf{n}}}{\sqrt{\mathbf{m}! \mathbf{n}!}} \Gamma(\boldsymbol{\alpha}, \boldsymbol{\beta})|_{\boldsymbol{\alpha}=\boldsymbol{\beta}=0}. \quad (10)$$

We now lump together the complex amplitudes and indices into single vectors

$$\boldsymbol{\nu} = \begin{bmatrix} \boldsymbol{\alpha} \\ \boldsymbol{\beta} \end{bmatrix} \in \mathbb{C}^{2\ell}, \quad (11)$$

$$\mathbf{k} = \begin{bmatrix} \mathbf{m} \\ \mathbf{n} \end{bmatrix} \in \mathbb{N}_0^{2\ell}, \quad (12)$$

so that we can express all of our calculations in terms of a single vector of amplitudes, including the generating function, which we now indicate as

$$\Gamma(\boldsymbol{\nu}) = \sum_{\mathbf{k}=0}^{\infty} \frac{\boldsymbol{\nu}^{\mathbf{k}}}{\sqrt{\mathbf{k}!}} \mathcal{G}_{\mathbf{k}}. \quad (13)$$

As shown in subsection II C, the generating function $\Gamma(\boldsymbol{\nu})$ for a Gaussian operator \mathcal{G} is in the exponential form

$\Gamma(\boldsymbol{\nu}) = C e^{Q(\boldsymbol{\nu})}$, which means that we can express high-order derivatives recursively, using only the derivatives at zero of the exponent $Q(\boldsymbol{\nu})$.

Furthermore, the exponent $Q(\boldsymbol{\nu})$ is a polynomial of degree 2, which we can write as:

$$Q(\boldsymbol{\nu}) = \boldsymbol{\mu}^T \boldsymbol{\nu} - \frac{1}{2} \boldsymbol{\nu}^T \boldsymbol{\Sigma} \boldsymbol{\nu}. \quad (14)$$

This means that all of its mixed derivatives of order higher than 2 vanish:

$$\partial_{\boldsymbol{\nu}}^{\mathbf{k}} Q(\boldsymbol{\nu})|_{\boldsymbol{\nu}=0} = 0 \text{ if } \sum_{i=1}^{2\ell} k_i > 2. \quad (15)$$

Because of this, all the derivatives of the exponent that we will ever need are those of degree 1 and 2:

$$\frac{\partial}{\partial \nu_i} Q(\boldsymbol{\nu})|_{\boldsymbol{\nu}=0} = \mu_i, \quad (16)$$

$$\frac{\partial^2}{\partial \nu_i \partial \nu_j} Q(\boldsymbol{\nu})|_{\boldsymbol{\nu}=0} = -\Sigma_{ij}. \quad (17)$$

Finally, note that although $\mathcal{G}_{\mathbf{k}}$ is a tensor of rank 2ℓ , for familiarity with the terminology we still refer to its elements as “matrix elements”.

B. Generating function for multimode Gaussian transformations

As a corollary of the Bloch-Messiah decomposition [20, 39], a general ℓ -mode Gaussian transformation can be parametrized as

$$\mathcal{G} = \mathcal{G}(\boldsymbol{\gamma}, \mathbf{W}, \boldsymbol{\zeta}, \mathbf{V}) = \mathcal{D}(\boldsymbol{\gamma}) \mathcal{U}(\mathbf{W}) \mathcal{S}(\boldsymbol{\zeta}) \mathcal{U}(\mathbf{V}), \quad (18)$$

where we used the notation $\mathcal{D}(\boldsymbol{\gamma}) = \bigotimes_{i=1}^{\ell} D_i(\gamma_i)$, $\mathcal{S}(\boldsymbol{\zeta}) = \bigotimes_{i=1}^{\ell} S_i(\zeta_i)$ for tensor products of single-mode displacement and squeezing operators defined by

$$D_j(\gamma_j) = \exp\left(\gamma_j a_j^\dagger - \text{H.c.}\right), \quad \gamma_j \in \mathbb{C}, \quad (19)$$

$$S_j(\zeta_j) = \exp\left(\frac{\zeta_j^*}{2} a_j^2 - \text{H.c.}\right), \quad \zeta_j = r_j e^{i\delta_j} \in \mathbb{C}. \quad (20)$$

Here we introduced the annihilation a_j and creation a_j^\dagger operators of the ℓ modes satisfying the canonical commutation relations

$$[a_j, a_l^\dagger] = \delta_{j,l}, \quad [a_j, a_l] = [a_j^\dagger, a_l^\dagger] = 0. \quad (21)$$

The Hilbert space operator $\mathcal{U}(\mathbf{V})$ represents a general multimode passive transformation (physically corresponding to an interferometer) and is parametrized by a unitary matrix \mathbf{V} that transforms the creation operators as

$$\mathcal{U}^\dagger(\mathbf{V}) a_i^\dagger \mathcal{U}(\mathbf{V}) = \sum_{l=1}^{\ell} V_{il}^* a_l^\dagger, \quad \mathcal{U}(\mathbf{V}) a_l^\dagger \mathcal{U}^\dagger(\mathbf{V}) = \sum_{i=1}^{\ell} V_{il} a_i^\dagger. \quad (22)$$

Using these definitions, in Appendix A we show the following:

$$e^{\frac{1}{2}[\|\boldsymbol{\alpha}\|^2 + \|\boldsymbol{\beta}\|^2]} \langle \boldsymbol{\alpha}^* | \mathcal{D}(\boldsymbol{\gamma}) \mathcal{U}(\mathbf{W}) \mathcal{S}(\boldsymbol{\zeta}) \mathcal{U}(\mathbf{V}) | \boldsymbol{\beta} \rangle = C \exp\left(\boldsymbol{\mu}^T \boldsymbol{\nu} - \frac{1}{2} \boldsymbol{\nu}^T \boldsymbol{\Sigma} \boldsymbol{\nu}\right), \quad (23)$$

where

$$C = \frac{\exp\left(-\frac{1}{2}[\|\boldsymbol{\gamma}\|^2 + \boldsymbol{\gamma}^\dagger \mathbf{W} \text{diag}(e^{i\delta} \tanh \mathbf{r}) \mathbf{W}^T \boldsymbol{\gamma}^*]\right)}{\sqrt{\prod_{i=1}^{\ell} \cosh r_i}}, \quad (24)$$

$$\boldsymbol{\mu}^T = \left[\boldsymbol{\gamma}^\dagger \mathbf{W} \text{diag}(e^{i\delta} \tanh \mathbf{r}) \mathbf{W}^T + \boldsymbol{\gamma}^T, -\boldsymbol{\gamma}^\dagger \mathbf{W} \text{diag}(\text{sech } \mathbf{r}) \mathbf{V}\right], \quad (25)$$

$$\boldsymbol{\Sigma} = \left[\begin{array}{c|c} \mathbf{W} \text{diag}(e^{i\delta} \tanh \mathbf{r}) \mathbf{W}^T & -\mathbf{W} \text{diag}(\text{sech } \mathbf{r}) \mathbf{V} \\ \hline -\mathbf{V}^T \text{diag}(\text{sech } \mathbf{r}) \mathbf{W}^T & -\mathbf{V}^T \text{diag}(e^{-i\delta} \tanh \mathbf{r}) \mathbf{V} \end{array} \right]. \quad (26)$$

With these results we are now ready to write explicit recurrence relations for the matrix elements of a general multimode Gaussian gate.

C. From generating functions to matrix elements

We use the recent result in [40] to express the matrix elements of the Gaussian operator recursively (see Appendix B):

$$\mathcal{G}_0 = C, \quad (27)$$

$$\mathcal{G}_{\mathbf{k}+1_i} = \frac{1}{\sqrt{k_i+1}} \sum_{j=0}^{\mathbf{k}} \sqrt{\frac{\mathbf{k}!}{j!}} \frac{1}{(\mathbf{k}-j)!} \mathcal{G}_j \partial_{\boldsymbol{\nu}}^{\mathbf{k}+1_i-j} Q(\boldsymbol{\nu})|_{\boldsymbol{\nu}=0}, \quad (28)$$

where $\mathbf{1}_i$ is a vector with all zeros and a single 1 at position i , and therefore to obtain the vector $\mathbf{k} + \mathbf{1}_i$ we take the vector \mathbf{k} and we increment k_i by 1.

We stress that Eq. (28) works for *any* generating function in exponential form. However, as mentioned above, in our case the exponent Q is a polynomial of degree 2, so the recurrence relation simplifies considerably because the derivative of Q is zero unless $\mathbf{j} = \mathbf{k}$ or $\mathbf{j} = \mathbf{k} - \mathbf{1}_l$ for some index l :

$$\mathcal{G}_{\mathbf{k}+1_i} = \frac{1}{\sqrt{k_i+1}} \left(\mathcal{G}_{\mathbf{k}} \mu_i - \sum_{l=1}^{2\ell} \sqrt{k_l} \mathcal{G}_{\mathbf{k}-1_l} \Sigma_{il} \right). \quad (29)$$

This, together with Eq. (82) which shows how to obtain gradients, is the primary result of our work.

As an example, we derive the two recurrence relations for the single mode case, i.e., $\ell = 1$. For convenience and ease of vectorization when programming, we can use the first relation to build the first column of the matrix and

the second relation to subsequently build the rows:

$$\mathcal{G}_{m+1,n} = \frac{1}{\sqrt{m+1}} \left(\mathcal{G}_{m,n}\mu_1 - \sqrt{m}\mathcal{G}_{m-1,n}\Sigma_{11} - \sqrt{n}\mathcal{G}_{m,n-1}\Sigma_{12} \right), \quad (30)$$

$$\mathcal{G}_{m,n+1} = \frac{1}{\sqrt{n+1}} \left(\mathcal{G}_{m,n}\mu_2 - \sqrt{m}\mathcal{G}_{m-1,n}\Sigma_{21} - \sqrt{n}\mathcal{G}_{m,n-1}\Sigma_{22} \right). \quad (31)$$

We represent this example pictorially in Fig. 1.

For Gaussian operators on ℓ modes, the recurrence relations allow us to combine $2\ell + 1$ neighbouring elements in 2ℓ different ways (by incrementing each of the 2ℓ indices) and generate 2ℓ new elements.

III. APPLICATIONS: SINGLE- AND TWO-MODE GATES AND PASSIVE GAUSSIAN TRANSFORMATIONS

All Gaussian single- and two-mode transformations will be expressed as a combination of four elementary operations: single-mode phase shifts, single-mode squeezing, single-mode displacement and beamsplitters. All of these elements are parametrized as follows: the phase rotation gate $R(\phi)$ depends on an angle ϕ , the single-mode squeezer $S(\zeta)$ depends on a single complex parameter which we express in polar form $\zeta = re^{i\delta}$, the displacement gate $D(\gamma)$ depends on a single complex parameter γ which we leave as is, and finally the beamsplitter $B(\theta, \varphi)$ depends on two angles (θ, φ) . Each gate is expressed as the exponential of mode operators. In particular, for the rotation and beamsplitter gates we write

$$R(\phi) = \exp(i\phi a^\dagger a), \quad (32)$$

$$B(\theta, \varphi) = \exp \left[\theta \left(e^{i\varphi} a_1 a_2^\dagger - e^{-i\varphi} a_1^\dagger a_2 \right) \right]. \quad (33)$$

For example, the 50/50 beam splitter with real coefficients corresponds to $(\theta, \varphi) = (\pi/4, 0)$. Note that the last two gates are special cases of a passive linear optical transformation, thus they can be written as $\mathcal{U}(\mathbf{W})$ where

$$\mathbf{W} = e^{i\phi}, \quad (34a)$$

$$\mathbf{W} = \begin{bmatrix} \cos \theta & -e^{-i\varphi} \sin \theta \\ e^{i\varphi} \sin \theta & \cos \theta \end{bmatrix}, \quad (34b)$$

respectively.

A. Single-mode Gaussian gate

A simple way to parametrize a general single-mode Gaussian operation is as follows:

$$\mathcal{G}^{(1)} = \mathcal{G}^{(1)}(\gamma, \phi, \zeta) = D(\gamma)R(\phi)S(\zeta). \quad (35)$$

By using Eq. (34a) and the general result from the last section we easily find

$$C = \frac{\exp \left(-\frac{1}{2} [|\gamma|^2 + \gamma^{*2} e^{i(\delta+2\phi)} \tanh r] \right)}{\sqrt{\cosh r}}, \quad (36)$$

$$\boldsymbol{\mu}^T = [\gamma^* e^{i(\delta+2\phi)} \tanh r + \gamma, -\gamma^* e^{i\phi} \operatorname{sech} r], \quad (37)$$

$$\boldsymbol{\Sigma} = \begin{bmatrix} e^{2i\varphi} e^{i\delta} \tanh r & -e^{i\phi} \operatorname{sech} r \\ -e^{i\phi} \operatorname{sech} r & e^{-i\delta} \tanh r \end{bmatrix}. \quad (38)$$

These values enter the recurrence relations (30) and (31), which are depicted in Fig. 1.

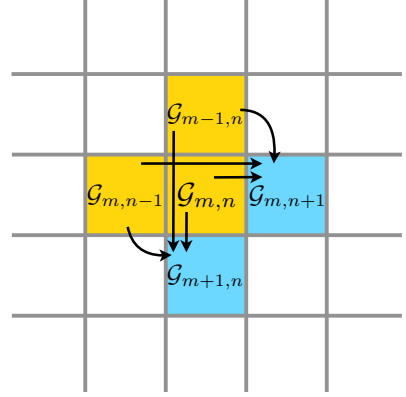


FIG. 1. The three neighbouring matrix elements shown in orange ($\mathcal{G}_{m-1,n}$, $\mathcal{G}_{m,n}$ and $\mathcal{G}_{m,n-1}$) can be linearly combined in two different ways to generate $\mathcal{G}_{m+1,n}$ or $\mathcal{G}_{m,n+1}$. These recurrence rules are also applicable at the edge of the matrix by considering “outer elements” as zeros. For Gaussian operators on ℓ modes, the recurrence rules allow us to combine $2\ell + 1$ neighbouring elements in 2ℓ different ways and generate 2ℓ new elements.

1. Special case: single-mode squeezing

For a single-mode squeezing operator, we have $\phi = 0$ and $\gamma = 0$, and thus

$$C = \sqrt{\operatorname{sech} r}, \quad (39)$$

$$\boldsymbol{\mu}^T = [0, 0], \quad (40)$$

$$\boldsymbol{\Sigma} = \begin{bmatrix} e^{i\delta} \tanh r & -\operatorname{sech} r \\ -\operatorname{sech} r & e^{-i\delta} \tanh r \end{bmatrix}. \quad (41)$$

The recurrence relations simplify accordingly, and we obtain the matrix elements of the single-mode squeezer $S_{m,n} = \langle m | S(\zeta) | n \rangle$:

$$S_{0,0} = \sqrt{\operatorname{sech} r}, \quad (42)$$

$$S_{m+1,0} = -\sqrt{\frac{m}{m+1}} S_{m-1,0} e^{i\delta} \tanh r, \quad (43)$$

$$S_{m,n+1} = \frac{1}{\sqrt{n+1}} (\sqrt{m} S_{m-1,n} \operatorname{sech} r + \sqrt{n} S_{m,n-1} e^{-i\delta} \tanh r), \quad (44)$$

where we have set $n = 0$ in the first recurrence relation so that it builds the first column, and we can use the second relation to build the rows.

Thanks to μ being zero, we do not need to include the middle matrix element at each step while filling out the matrix, as depicted in Fig. 2. This gives rise to the typical checkerboard pattern of the squeezer matrix.

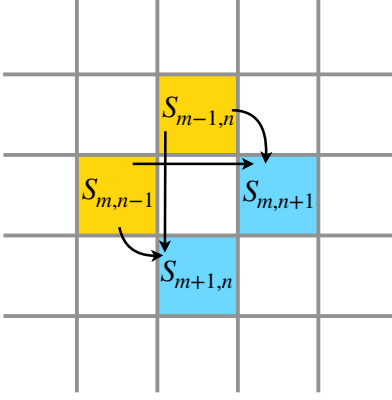


FIG. 2. When generating the single-mode squeezer matrix, two matrix elements are sufficient to generate another two at each step. Notice how this produces the checkerboard pattern of zeros that is typical of the squeezer matrix.

2. Special case: displacement

For a single-mode displacement operator, we have $\phi = 0$ and $\zeta = 0$ and therefore $\tanh r = 0$ and $\text{sech } r = 1$ and we find

$$C = e^{-\frac{1}{2}|\gamma|^2}, \quad (45)$$

$$\mu^T = [\gamma, -\gamma^*], \quad (46)$$

$$\Sigma = \begin{bmatrix} 0 & -1 \\ -1 & 0 \end{bmatrix}. \quad (47)$$

The recurrence relations simplify accordingly, and we obtain the matrix elements of the single-mode displacement operator $D_{m,n} = \langle m|D(\gamma)|n\rangle$:

$$D_{0,0} = e^{-\frac{|\gamma|^2}{2}}, \quad (48)$$

$$D_{m+1,0} = \frac{\gamma}{\sqrt{m+1}} D_{m,0}, \quad (49)$$

$$D_{m,n+1} = -\frac{\gamma^*}{\sqrt{n+1}} D_{m,n} + \sqrt{\frac{m}{n+1}} D_{m-1,n}. \quad (50)$$

Thanks to the diagonal of Σ being zero, also in this case each step is simplified, as depicted in Fig. 3.

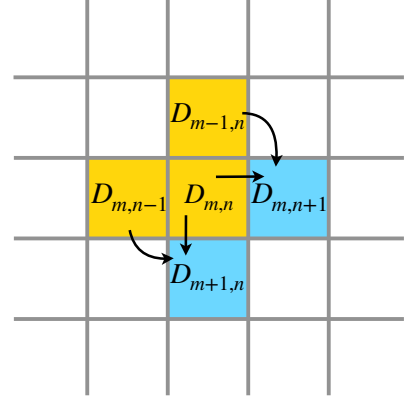


FIG. 3. When generating the single-mode displacement matrix, we only need two matrix elements to generate each new element along columns or rows.

B. Two-mode Gaussian gate

We can write the most general two-mode Gaussian transformation as

$$\mathcal{G}^{(2)} = \mathcal{D}(\gamma)\mathcal{R}(\phi)B(\theta', \varphi')S(\zeta)B(\theta, \varphi), \quad (51)$$

where $\phi = [\phi_1, \phi_2]$, $\gamma = [\gamma_1, \gamma_2]$ and $\zeta = [\zeta_1, \zeta_2]$ and where the single-mode gates factorize over the two modes. This gives a total of 14 real parameters (counting double for complex parameters), in accordance with Ref. [41]. The equations above can be recast into the form of Eq. (18) by writing $\mathcal{U}(\mathbf{V}) = B(\theta, \varphi)$ and $\mathcal{U}(\mathbf{W}) = \mathcal{R}(\phi)B(\theta', \varphi')$, with

$$\mathbf{V} = \begin{bmatrix} \cos \theta & -e^{-i\varphi} \sin \theta \\ e^{i\varphi} \sin \theta & \cos \theta \end{bmatrix}, \quad (52)$$

$$\mathbf{W} = \begin{bmatrix} e^{i\phi_1} & 0 \\ 0 & e^{i\phi_2} \end{bmatrix} \begin{bmatrix} \cos \theta' & -e^{-i\varphi'} \sin \theta' \\ e^{i\varphi'} \sin \theta' & \cos \theta' \end{bmatrix}. \quad (53)$$

1. Special case: Two-mode squeezer

The two-mode squeezer is defined as $S^{(2)}(\zeta) = \exp(\zeta a_1^\dagger a_2^\dagger - \text{H.c.})$ and can be decomposed in terms of beamsplitters and single-mode squeezing operations as follows:

$$S^{(2)}(z) = B(-\pi/4, 0) [S(\zeta) \otimes S(-\zeta)] B(\pi/4, 0). \quad (54)$$

From the decomposition above one easily finds:

$$C = \text{sech } r, \quad (55)$$

$$\boldsymbol{\mu}^T = [0, 0], \quad (56)$$

$$\boldsymbol{\Sigma} = \quad (57)$$

$$\begin{bmatrix} 0 & -e^{i\delta} \tanh r & -\text{sech } r & 0 \\ -e^{i\delta} \tanh r & 0 & 0 & -\text{sech } r \\ -\text{sech } r & 0 & 0 & e^{-i\delta} \tanh r \\ 0 & -\text{sech } r & e^{-i\delta} \tanh r & 0 \end{bmatrix}.$$

Note that a two-mode squeezing operation creates photons in pairs, which implies that the difference of photon number between the two modes is conserved. This observation is mathematically equivalent to the fact that that the operation has an $SU(1, 1)$ symmetry [42]. If we write $S_{m,n,p,q}^{(2)} = \langle m, n | S_2(z) | p, q \rangle$ then the only nonzero elements of this tensor satisfy $m - n = p - q$. Matrix elements that do not satisfy this selection rule are zero and we can construct the whole rank-4 tensor by looping over at most 3 indices:

$$S_{0,0,0,0}^{(2)} = \text{sech } r, \quad (58)$$

$$S_{n,n,0,0}^{(2)} = -S_{n-1,n-1,0,0}^{(2)} \Sigma_{1,2}, \quad (59)$$

$$S_{m,n,m-n,0}^{(2)} = -\sqrt{\frac{m}{m-n}} S_{m-1,n,m-n-1,0}^{(2)} \Sigma_{1,3}, \quad (60)$$

$$S_{m,n,p,p-(m-n)}^{(2)} = \frac{-1}{\sqrt{p-(m-n)}} \times \left(\sqrt{n} S_{m,n-1,p,p-(m-n)-1}^{(2)} \Sigma_{2,4} + \sqrt{p} S_{m,n,p-1,p-(m-n)-1}^{(2)} \Sigma_{3,4} \right). \quad (61)$$

C. Passive Gaussian Transformations: Interferometers

These ℓ -mode transformations, which correspond to interferometers parametrized by an $\ell \times \ell$ unitary matrix \mathbf{V} , can be obtained from our general results by setting $\boldsymbol{\zeta} = \boldsymbol{\delta} = \mathbf{0}$ and selecting, without loss of generality, $\mathbf{W} = \mathbb{I}$ to obtain

$$C = 1, \quad (62)$$

$$\boldsymbol{\mu}^T = \mathbf{0}, \quad (63)$$

$$\boldsymbol{\Sigma} = - \left[\begin{array}{c|c} \mathbf{0} & \mathbf{V} \\ \hline \mathbf{V}^T & \mathbf{0} \end{array} \right]. \quad (64)$$

We can write $\langle \mathbf{m} | \mathcal{U}(\mathbf{V}) | \mathbf{n} \rangle = U_{\mathbf{m},\mathbf{n}}$ and write the following recurrence relations

$$U_{\mathbf{0},\mathbf{0}} = 1, \quad (65a)$$

$$U_{\mathbf{m}+1_i,\mathbf{n}} = \frac{1}{\sqrt{m_i+1}} \sum_{j=1}^{\ell} V_{i,j} \sqrt{n_j} U_{\mathbf{m},\mathbf{n}-1_j}, \quad (65b)$$

$$U_{\mathbf{m},\mathbf{n}+1_i} = \frac{1}{\sqrt{n_i+1}} \sum_{j=1}^{\ell} V_{j,i} \sqrt{m_j} U_{\mathbf{m}-1_j,\mathbf{n}}. \quad (65c)$$

These equations have a particular simple physical interpretation: they tell us that to scatter off one additional photon in the bra side $\mathbf{m} + 1_i$ one photon has to be sent into the interferometer in the ket side $\mathbf{n} - 1_j$. In particular, we find that the probability amplitude that a single photon injected in port j ends up in port i is precisely the (i, j) entry of the unitary matrix describing the interferometer:

$$U_{1_i,1_j} = V_{i,j}. \quad (66)$$

Note that $U_{\mathbf{m},\mathbf{n}}$ is nonzero only if $\sum_{i=1}^{\ell} m_i = \sum_{i=1}^{\ell} n_i$ since interferometers do not create or destroy particles (mathematically, this is because they have $U(n)$ symmetry). Matrix elements that do not satisfy this selection rule are zero and we can construct the whole rank- 2ℓ tensor by looping over at most $2\ell - 1$ indices. Let us illustrate this for a beamsplitter, which is a special case of a general passive transformation, and for which \mathbf{V} is of size 2×2 and given in Eq. (52). The recurrence relations we find are:

$$B_{0,0,0} = 1, \quad (67)$$

$$B_{m,n,m+n,0} = \frac{1}{\sqrt{m+n}} \left(\sqrt{m} V_{1,1} B_{m-1,n,m+n-1,0} + \sqrt{n} V_{2,1} B_{m,n-1,m+n-1,0} \right), \quad (68)$$

$$B_{m,n,p,m+n-p} = \frac{1}{\sqrt{m+n-p}} \times \left(\sqrt{m} V_{1,2} B_{m-1,n,p,m+n-p-1} + \sqrt{n} V_{2,2} B_{m,n-1,p,m+n-p-1} \right), \quad (69)$$

where $\langle m, n | B(\theta, \phi) | p, q \rangle = B_{m,n,p,q}$.

IV. RECURSIVE GRADIENTS

In this section we present recurrence relations to construct the gradients of Gaussian operators with respect to their parameters. Gradients are essential in optimization procedures, such as the optimization of a whole circuit built out of several operators. The action of a circuit on input states is determined by the parameters of the

various operators that it contains, and the optimal circuit is achieved by an optimal choice of parameters. The optimization procedure starts by initializing the parameters randomly (usually with very small values) and then slowly varies them until we obtain a circuit that is similar enough to the optimal one.

In order to carry out this optimization, we define a function that evaluates the cost or “loss” associated with the current parameter values. By design, the optimal choice of parameters corresponds to the global minimum of the loss function. Our goal is then to minimize the loss by slowly varying the parameters in a sequence of steps via the gradient descent algorithm (or one of its variants). In order to run this algorithm, we need to backpropagate the gradient of the loss function using the chain rule, all the way back to reach each of the parameters, obtaining therefore the rate of change of the loss with respect to the parameters, which tells us how to update their values and decrease the loss.

In the next subsections we explain how to correctly handle the gradient of complex and real parameters, show that gradients can be easily computed from the matrix representation of the operators and give some examples.

A. Gradients with respect to complex parameters

For a complex parameter ξ , the gradient-descent update step should use the partial derivative of a real loss function L with respect to the *conjugate* of the parameter [43]:

$$\xi \leftarrow \xi - \eta \frac{\partial L}{\partial \xi^*}. \quad (70)$$

Clearly, this update rule falls back to the regular rule in the case of a real parameter. To compute the gradient for the update, we need to treat complex variables and their conjugate as *independent* variables, which allows us to compute gradients of non-holomorphic functions [43]. The chain rule then looks as follows:

$$\frac{\partial L}{\partial \xi^*} = \sum_{\mathbf{k}} \frac{\partial L}{\partial \mathcal{G}_{\mathbf{k}}^*} \frac{\partial \mathcal{G}_{\mathbf{k}}^*}{\partial \xi^*} + \frac{\partial L}{\partial \mathcal{G}_{\mathbf{k}}} \frac{\partial \mathcal{G}_{\mathbf{k}}}{\partial \xi^*}. \quad (71)$$

In an automatic differentiation framework such as TensorFlow or PyTorch, if we wish to customize the computation of the gradient of a new operation (e.g., when the new operation makes use of compiled code which is treated like a black box) we are supplied with the upstream gradient tensor $\partial L / \partial \mathcal{G}_{\mathbf{k}}^*$. It is our task to combine it with the local gradients $\partial \mathcal{G}_{\mathbf{k}} / \partial \xi^*$ and $\partial \mathcal{G}_{\mathbf{k}}^* / \partial \xi^*$ as prescribed by the chain rule, to produce the downstream gradient $\partial L / \partial \xi^*$.

In order to obtain the various parts of Eq. (71) we proceed as follows: for the first part of (71), the upstream gradient tensor $\partial L / \partial \mathcal{G}_{\mathbf{k}}^*$ is given to us by the software so

we only have to compute the local gradient:

$$\frac{\partial \mathcal{G}_{\mathbf{k}}^*}{\partial \xi^*} = \left(\frac{\partial \mathcal{G}_{\mathbf{k}}}{\partial \xi} \right)^*. \quad (72)$$

For the second part of (71) we can conjugate the upstream gradient tensor (as the loss function is real):

$$\frac{\partial L}{\partial \mathcal{G}_{\mathbf{k}}} = \left(\frac{\partial L}{\partial \mathcal{G}_{\mathbf{k}}^*} \right)^*, \quad (73)$$

but as the matrix elements of $\mathcal{G}_{\mathbf{k}}$ are complex and non-holomorphic functions of ξ , their derivatives with respect to ξ and ξ^* are independent and we need to compute $\partial \mathcal{G}_{\mathbf{k}} / \partial \xi^*$ separately. On the other hand, for a real parameter x computing a single gradient tensor $\frac{\partial \mathcal{G}_{\mathbf{k}}}{\partial x}$ would suffice:

$$\frac{\partial L}{\partial x} = \sum_{\mathbf{k}} \frac{\partial L}{\partial \mathcal{G}_{\mathbf{k}}^*} \frac{\partial \mathcal{G}_{\mathbf{k}}^*}{\partial x} + \frac{\partial L}{\partial \mathcal{G}_{\mathbf{k}}} \frac{\partial \mathcal{G}_{\mathbf{k}}}{\partial x} \quad (74)$$

$$= 2\Re \left(\sum_{\mathbf{k}} \frac{\partial L}{\partial \mathcal{G}_{\mathbf{k}}} \frac{\partial \mathcal{G}_{\mathbf{k}}}{\partial x} \right), \quad (75)$$

as in this case $\frac{\partial \mathcal{G}_{\mathbf{k}}^*}{\partial x}$ and $\frac{\partial \mathcal{G}_{\mathbf{k}}}{\partial x}$ are the conjugate of each other. If one prefers to have only real parameters then there is an additional step: one can write each complex parameter in Cartesian or polar form, and then treat each of these as an additional function of two real variables, e.g., for $\xi = r e^{i\phi}$:

$$\frac{\partial L}{\partial r} = 2\Re \left(\frac{\partial L}{\partial \xi^*} \frac{\partial \xi^*}{\partial r} \right) = 2\Re \left(\frac{\partial L}{\partial \xi^*} e^{-i\phi} \right), \quad (76)$$

$$\frac{\partial L}{\partial \phi} = 2\Re \left(\frac{\partial L}{\partial \xi^*} \frac{\partial \xi^*}{\partial \phi} \right) = -2\Re \left(\frac{\partial L}{\partial \xi^*} i \xi^* \right). \quad (77)$$

Furthermore, if the gate depends on a single parameter (real or complex) more simplifications can be made as shown in Appendix C.

B. Computing gradients with the generating function method

An ℓ -mode Gaussian gate has $2\ell^2 + 3\ell$ real parameters (counting double for complex parameters), therefore in order to obtain all the parameter updates we need to compute $2\ell^2 + 3\ell$ derivatives, some of which will be combined to form the parameter updates of the complex parameters.

Another key insight of the generating function method is that to compute the gradients of the matrix elements we can simply differentiate the generating function with respect to the parameters *before* computing the high-order derivatives (here with respect to a generic param-

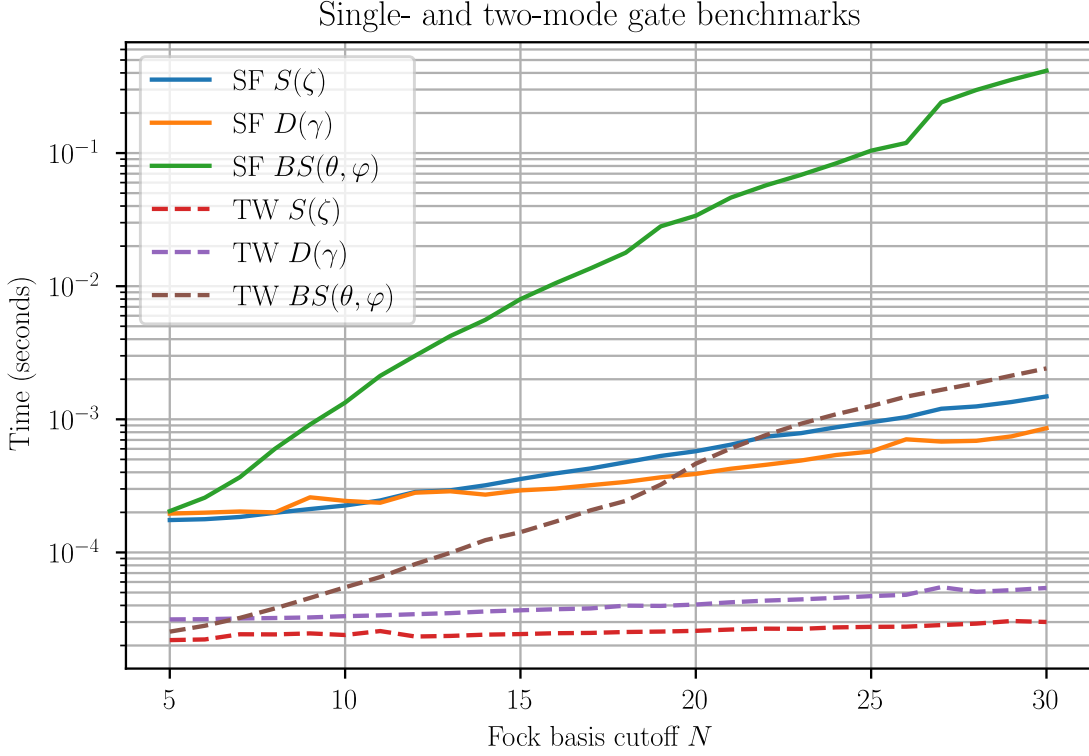


FIG. 4. Benchmarks for the computation of the squeezing $S(\zeta)$, displacement $D(\gamma)$ and beamsplitter $B(\theta, \varphi)$ gates using **Strawberry Fields** (SF) 0.12.1 and the methods from this work as implemented in **The Walrus** (TW). Note that for a cutoff of $N = 30$ our implementations are two orders of magnitude faster. Finally, we also benchmarked the two-mode squeezing gate; the times we find for our implementation are visually indistinguishable from the ones for our beamsplitter, reflecting the fact that both gates can be implemented by looping over three indices despite being rank-4 tensors. The benchmarks in this figure were performed on a single core of an Intel-i5 processor @ 2.50 GHz.

eter ξ):

$$\partial_\xi \mathcal{G}_{\mathbf{k}} = \frac{\partial_{\nu}^{\mathbf{k}}}{\sqrt{\mathbf{k}!}} \partial_\xi \Gamma(\nu)|_{\nu=0} = \frac{\partial_{\nu}^{\mathbf{k}}}{\sqrt{\mathbf{k}!}} \partial_\xi C e^{Q(\nu)}|_{\nu=0} \quad (78)$$

$$\begin{aligned} &= \frac{\partial_{\nu}^{\mathbf{k}}}{\sqrt{\mathbf{k}!}} \Gamma(\nu) \left(\frac{\partial_\xi C}{C} + \partial_\xi Q(\nu) \right) |_{\nu=0} \quad (79) \\ &= \frac{\partial_{\nu}^{\mathbf{k}}}{\sqrt{\mathbf{k}!}} \Gamma(\nu) \left(\frac{\partial_\xi C}{C} + \frac{\partial \mu^T}{\partial \xi} \nu - \frac{1}{2} \nu^T \frac{\partial \Sigma}{\partial \xi} \nu \right) \Big|_{\nu=0}. \end{aligned} \quad (80)$$

Expression (80) contains terms proportional to $\nu^n \Gamma(\nu)$, whose derivative can be expressed using the elements of $\mathcal{G}_{\mathbf{k}}$:

$$\frac{\partial_{\nu}^{\mathbf{k}}}{\sqrt{\mathbf{k}!}} \nu^n \Gamma(\nu)|_{\nu=0} = \sqrt{(\mathbf{k})_n} \mathcal{G}_{\mathbf{k}-\mathbf{n}}, \quad (81)$$

where $(k)_n = k(k-1)(k-2) \dots (k-n+1)$ is the Pochhammer symbol and $(\mathbf{k})_n = \prod_i (k_i)_{n_i}$ (with the convention that $(k)_0 = 1$). So once we compute the tensor representation of a Gaussian operator, we can use it to compute its gradient with respect to a parametrization. Continu-

ing from Eq. (80) we can write:

$$\begin{aligned} \frac{\partial \mathcal{G}_{\mathbf{k}}}{\partial \xi} &= \frac{\partial_\xi C}{C} \mathcal{G}_{\mathbf{k}} + \sum_i \frac{\partial \mu_i}{\partial \xi} \sqrt{k_i} \mathcal{G}_{\mathbf{k}-1_i} \\ &\quad - \sum_{i>j} \frac{\partial \Sigma_{ij}}{\partial \xi} \sqrt{k_i k_j} \mathcal{G}_{\mathbf{k}-1_i-1_j} \\ &\quad - \sum_i \frac{\partial \Sigma_{ii}}{\partial \xi} \sqrt{k_i(k_i-1)} \mathcal{G}_{\mathbf{k}-2_i}. \end{aligned} \quad (82)$$

This, together with Eq. (29), is the main result of our work.

As an example, we show the derivatives of the single mode Gaussian operator with respect to the complex displacement parameter γ and γ^* (recall that we must treat them as independent variables). We begin by differenti-

ating C , μ and Σ :

$$\frac{\partial_\gamma C}{C} = -\frac{\gamma^*}{2}, \quad (83)$$

$$\frac{\partial_{\gamma^*} C}{C} = -\frac{\gamma}{2} - \frac{1}{2}\gamma^* e^{i(\delta+2\phi)} \tanh r, \quad (84)$$

$$\frac{\partial \mu}{\partial \gamma} = [1, 0], \quad (85)$$

$$\frac{\partial \mu}{\partial \gamma^*} = [e^{i(\delta+2\phi)} \tanh r, -e^{i\phi} \operatorname{sech} r], \quad (86)$$

$$\frac{\partial \Sigma}{\partial \gamma} = \mathbf{0}, \quad (87)$$

$$\frac{\partial \Sigma}{\partial \gamma^*} = \mathbf{0}. \quad (88)$$

Therefore, the gradients of the matrix elements are:

$$\frac{\partial \mathcal{G}_{m,n}}{\partial \gamma} = -\frac{\gamma^*}{2} \mathcal{G}_{m,n} + \sqrt{m} \mathcal{G}_{m-1,n}, \quad (89)$$

$$\begin{aligned} \frac{\partial \mathcal{G}_{m,n}}{\partial \gamma^*} = & -\left(\frac{\gamma}{2} + \frac{1}{2}\gamma^* e^{i(\delta+2\phi)} \tanh r\right) \mathcal{G}_{m,n} \\ & + e^{i(\delta+2\phi)} \sqrt{m} \mathcal{G}_{m-1,n} \tanh r \\ & - e^{i\phi} \sqrt{n} \mathcal{G}_{m,n-1} \operatorname{sech} r. \end{aligned} \quad (90)$$

We then combine both of these expressions with the upstream gradient $\partial L / \partial \mathcal{G}_{mn}^*$ and its conjugate as prescribed in Eq. (71) to obtain the single gradient for the update, $\partial L / \partial \gamma^*$. We proceed in an analogous way for all the other parameters.

V. NUMERICAL EXPERIMENTS

In this section we present a series of experiments that show the effectiveness of our method. First, we benchmark our methods and implementations for the displacement, squeezing and beamsplitter gate against the implementations of **Strawberry Fields** (SF) version 0.12.1. We note that as of version 0.13, SF uses the methods presented here and implemented in **The Walrus**. The results of the benchmarks are summarized in Fig. 4; our implementations are two orders of magnitude faster than the ones in SF 0.12.1, and are also more stable and memory efficient. For example, if one tries to calculate a displacement gate by using its known expansion in terms of Laguerre polynomials [23] it is necessary to perform divisions by the factorial of the number of photons n , which results in numerical overflows for $n \sim 100$. Our explicit recurrence relations avoid completely this issue for any number of modes.

Second, we compare our methods against the implementations of the beamsplitter in the package **Bosonic**[8]. This package has a hard-coded cutoff of 11. We benchmark up to this cutoff in Fig. 5. Even for these modest sizes our implementation achieves almost two orders of magnitude in improvement.

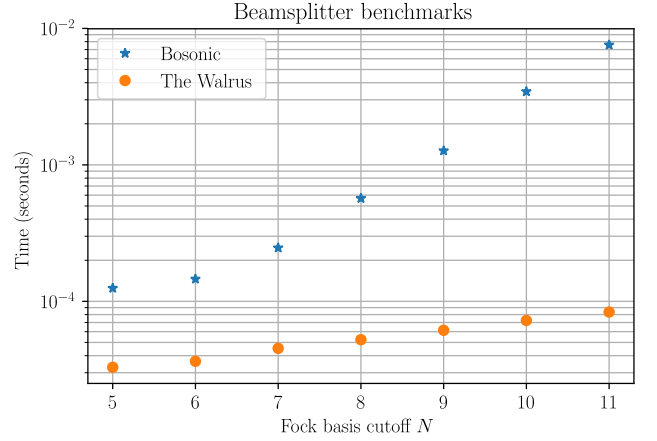


FIG. 5. Benchmarks for the computation of the beamsplitter $BS(\theta, \varphi)$ using **Bosonic** and the methods from this work as implemented in **The Walrus**. Note that for a given cutoff N , **Bosonic** calculates $\mathcal{B}_{i,j}^{(N)} = \langle N-i, i | BS(\theta, \varphi) | N-j, j \rangle$ and that in their implementation the constraint $N \leq 11$ is hard-coded. For a fair comparison we benchmark their code against a wrapper function that calculates the tensor $\langle m, n | BS(\theta, \varphi) | k, l \rangle$ and then constructs the relevant matrix $\mathcal{B}_{i,j}^{(N)}$ from it. Note that our methods offer a very significant improvement in speed even for the modest cutoff considered here. The benchmarks in this figure were performed on a single core of an Intel-i5 processor @ 2.50 GHz.

Third, we test a circuit optimization task. We start by setting up a circuit built by alternating single-mode Gaussian gates and single-mode Kerr gates. A Kerr gate is a non-linear optical interaction which varies the phase of a Fock state according to the square of the occupation number:

$$K(\kappa) = e^{i\kappa(a^\dagger a)^2}, \quad (91)$$

and is therefore diagonal in the photon number basis. Such single-mode circuit corresponds to a unitary transformation which we can write as a stack of M layers:

$$U(\gamma, \phi, \zeta) = \prod_{m=1}^M \mathcal{G}^{(1)}(\gamma_m, \phi_m, \zeta_m) K(\kappa_m). \quad (92)$$

We then input the single-mode vacuum state $|0\rangle$ and optimize the parameters such that the unitary $U(\gamma, \phi, \zeta)$ produces an output as close as possible to the desired target state. We choose three target states: a single photon state $|1\rangle$, an “ON” state, i.e. a superposition of the vacuum and a Fock state, in our case $(|0\rangle + |9\rangle)/\sqrt{2}$ and finally a Hex GKP state, which is a logical state of the single-mode GKP error correcting code [44]. To evaluate the quality of the state produced by the circuit we define a loss function between the output $U|0\rangle$ and the target:

$$L(|\psi_{\text{out}}\rangle) = -|\langle \psi_{\text{out}} | \psi_{\text{target}} \rangle|. \quad (93)$$

For the optimization we run the adaptive gradient descent algorithm **Adam**.

The results are presented in Table I and can be compared with the ones in table I of Ref. [5] (reported in parenthesis where they differ from ours). Our method allows us to use much higher cutoff dimensions, leading to equal or better fidelities in a significantly shorter time. The optimization of the Hex GKP state is particularly striking, as it reached better results in a fraction of the time while running on much slower hardware.

We point out that even if the final output has to contain few photons, using a large cutoff is beneficial because it allows intermediate layers to explore higher excitation numbers, which may be necessary to reach the desired output with high fidelity.

<i>Hyperparams</i>	<i>Single photon</i>	<i>ON</i>	<i>Hex GKP</i>
Cutoff N	100 (8)	100 (14)	100 (50)
Layers M	8	20	35 (25)
Steps	1500 (5000)	2500 (5000)	5000 (10000)
<i>Results</i>			
Fidelity	99.998%	99.995 (99.93)%	99.83 (99.60)%
Runtime (s)	50 (65)	260 (436)	720 (6668)

TABLE I. Optimization results for state generation. We indicate in parenthesis the values from Table I in Ref. [5] if they differ from ours. Thanks to the improved speed of our recursive algorithm we can push the cutoff to $N = 100$ and we can increase the number of layers for the generation of the Hex GKP state. Compared to the results in Table I of Ref. [5] we can either reach the same fidelity with fewer steps or overall better results (higher fidelity, fewer steps, shorter runtime). All of these optimizations have been run on a single core of an Intel Core i5 @ 3,1 GHz. For comparison the results in Ref. [5] are obtained in hardware of comparable speed for the first two target states and on a 20-core Intel Xeon CPU @ 2.4GHz with 252GB RAM for the Hex GKP state.

VI. CONCLUSIONS

We have presented a unified procedure for obtaining the Fock representation of a quantum optical Gaussian transformation using generating functions. From the generating functions we obtain recurrence relations which allow us to compute the matrix elements of any given Gaussian transformation when written in terms of its Bloch-Messiah decomposition. Furthermore, we have developed general techniques to also obtain the gradients of a given transformation once it is parametrized.

As particular examples we derived explicit recurrence relations for the displacement, single- and two-mode squeezing gates and the beamsplitter. These recurrence relations are part of the `fock_gradients` module of **The Walrus** written in pure Python using `Numpy` and are sped up using the just-in-time compiling capabilities of `Numba`. Our highly portable implementation makes our algorithms ideal for high performance simulation of quantum optical circuits using both CPUs and GPUs. Furthermore, we expect them to accelerate the research on quantum hardware, quantum machine learning, optical data processing, device discovery and device design.

Note added – While preparing this manuscript we became aware of related work by J. Huh [45].

ACKNOWLEDGEMENTS

N.Q. thanks S. Hossain, T. Isacsson, J. Izaac, N. Kiloran and A. Száva for valuable discussions. The authors also thank the open source scientific computing community, in particular the developers of `Numpy` [46], `Scipy` [47], `Jupyter` [48], `Matplotlib` [49] and `Numba` [50], without whom this research would not have been possible.

Appendix A: Multimode generating function

In Barnett and Radmore [22] (cf. Sec. 3.7 and Appendix 5) the following identities are proven:

$$\exp(\theta a^\dagger a) = : \exp([\exp(\theta) - 1] a^\dagger a) := \sum_{n=0}^{\infty} \frac{[\exp(\theta) - 1]^n a^{\dagger n} a^n}{n!}, \quad (\text{A1})$$

and also

$$\begin{aligned} S(\zeta) &= \exp\left(\frac{1}{2}\zeta^* a^2 - \text{H.c.}\right) = \exp\left(\frac{1}{2}r e^{-i\delta} a^2 - \text{H.c.}\right) \\ &= \exp\left(-\frac{\tanh r}{2} e^{i\delta} a^{\dagger 2}\right) \exp\left(-\left[a^\dagger a + \frac{1}{2}\right] \log \cosh r\right) \exp\left(\frac{\tanh r}{2} e^{i\delta} a^2\right). \end{aligned} \quad (\text{A2})$$

where we wrote $\zeta = r e^{i\delta}$. Putting these two identities together we can normal order a squeezing operator

$$\exp\left(\frac{1}{2}r e^{-i\delta} a^2 - \text{H.c.}\right) = \exp\left(-\frac{\tanh r}{2} e^{i\delta} a^{\dagger 2}\right) \times \frac{: \exp([\text{sech } r - 1] a^\dagger a) :}{\sqrt{\cosh r}} \times \exp\left(\frac{\tanh r}{2} e^{i\delta} a^2\right). \quad (\text{A3})$$

Using this expression one can find the matrix element of the squeezing operation between two coherent states

$$\langle \alpha^* | \exp \left(\frac{1}{2} r e^{-i\delta} a^2 - \text{H.c.} \right) | \beta \rangle = \frac{1}{\sqrt{\cosh r}} \langle \alpha^* | \beta \rangle \exp \left(-\frac{\tanh r}{2} e^{i\delta} \alpha^2 + [\text{sech } r - 1] \alpha \beta + \frac{\tanh r}{2} e^{-i\delta} \beta^2 \right), \quad (\text{A4})$$

and noting that

$$\langle \alpha^* | \beta \rangle = \exp \left(-\frac{1}{2} [|\alpha|^2 + |\beta|^2 - 2\alpha\beta] \right), \quad (\text{A5})$$

one can write

$$\langle \alpha^* | \exp \left(\frac{1}{2} r e^{i\delta} a^2 - \text{H.c.} \right) | \beta \rangle = \frac{\exp \left(-\frac{1}{2} [|\alpha|^2 + |\beta|^2] \right)}{\sqrt{\cosh r}} \exp \left(-\frac{1}{2} [\alpha \ \beta] \begin{bmatrix} e^{i\delta} \tanh r & -\text{sech } r \\ -\text{sech } r & -e^{-i\delta} \tanh r \end{bmatrix} \begin{bmatrix} \alpha \\ \beta \end{bmatrix} \right). \quad (\text{A6})$$

This proof generalizes in a straightforward way to

$$\langle \alpha^* | \mathcal{S}(\zeta) | \beta \rangle = \frac{\exp \left(-\frac{1}{2} [||\alpha||^2 + ||\beta||^2] \right)}{\sqrt{\prod_{i=1}^{\ell} \cosh r_i}} \exp \left(-\frac{1}{2} [\alpha \ \beta] \left[\begin{array}{c|c} \text{diag}(e^{i\delta} \tanh \mathbf{r}) & -\text{diag}(\text{sech } \mathbf{r}) \\ \hline -\text{diag}(\text{sech } \mathbf{r}) & -\text{diag}(e^{-i\delta} \tanh \mathbf{r}) \end{array} \right] \begin{bmatrix} \alpha \\ \beta \end{bmatrix} \right),$$

where $\zeta_j = r_j e^{i\delta_j}$.

From the definitions in Eq. (22) it is direct to show that

$$\mathcal{U}(\mathbf{V})|\beta\rangle = |\mathbf{V}\beta\rangle \text{ and } \langle \alpha^* | \mathcal{U}(\mathbf{W}) = \langle \mathbf{W}^\dagger \alpha^*|. \quad (\text{A7})$$

Finally, let us note that

$$\langle \alpha^* | \mathcal{D}(\gamma) = \langle \alpha^* - \gamma | \exp \left(\frac{1}{2} [\alpha^T \gamma - \gamma^\dagger \alpha^*] \right). \quad (\text{A8})$$

To show this last identity recall that $\langle \alpha^* | = \langle \mathbf{0} | \mathcal{D}(-\alpha^*)$ and use the composition rule for displacement operators (cf. Eq. 3.6.30 of Ref. [22]). With this setup we are finally ready to prove Eq. 23 as follows:

$$\langle \alpha^* | \mathcal{D}(\gamma) \mathcal{U}(\mathbf{W}) \mathcal{S}(\zeta) \mathcal{U}(\mathbf{V}) | \beta \rangle \quad (\text{A9a})$$

$$= \exp \left(\frac{1}{2} [\alpha^T \gamma - \gamma^\dagger \alpha^*] \right) \langle \alpha^* - \gamma | \mathcal{U}(\mathbf{W}) \mathcal{S}(\zeta) | \mathbf{V}\beta \rangle \quad (\text{A9b})$$

$$= \exp \left(\frac{1}{2} [\alpha^T \gamma - \gamma^\dagger \alpha^*] \right) \langle \mathbf{W}^\dagger (\alpha^* - \gamma) | \mathcal{S}(\zeta) | \mathbf{V}\beta \rangle \quad (\text{A9c})$$

$$= \frac{\exp \left(\frac{1}{2} [\alpha^T \gamma - \gamma^\dagger \alpha^*] \right)}{\sqrt{\prod_{i=1}^{\ell} \cosh r_i}} \exp \left(-\frac{1}{2} [||\alpha^* - \gamma||^2 + |\beta|^2] \right) \times \quad (\text{A9d})$$

$$\exp \left(-\frac{1}{2} [(\alpha^T - \gamma^\dagger) \mathbf{W}, \ \beta^T \mathbf{V}^T] \left[\begin{array}{c|c} \text{diag}(e^{i\delta} \tanh \mathbf{r}) & -\text{diag}(\text{sech } \mathbf{r}) \\ \hline -\text{diag}(\text{sech } \mathbf{r}) & -\text{diag}(e^{-i\delta} \tanh \mathbf{r}) \end{array} \right] \begin{bmatrix} \mathbf{W}^T (\alpha - \gamma^*) \\ \mathbf{V}\beta \end{bmatrix} \right).$$

At this point we introduce the symmetric, complex-unitary matrix

$$\Sigma = \left[\begin{array}{c|c} \mathbf{W} \text{diag}(e^{i\delta} \tanh \mathbf{r}) \mathbf{W}^T & -\mathbf{W} \text{diag}(\text{sech } \mathbf{r}) \mathbf{V} \\ \hline -\mathbf{V}^T \text{diag}(\text{sech } \mathbf{r}) \mathbf{W}^T & -\mathbf{V}^T \text{diag}(e^{-i\delta} \tanh \mathbf{r}) \mathbf{V} \end{array} \right] \quad (\text{A10})$$

$$= \left[\begin{array}{c|c} \mathbf{W} & \mathbf{0} \\ \hline \mathbf{0} & \mathbf{V}^T \end{array} \right] \left[\begin{array}{c|c} \text{diag}(e^{i\delta} \tanh \mathbf{r}) & -\text{diag}(\text{sech } \mathbf{r}) \\ \hline -\text{diag}(\text{sech } \mathbf{r}) & -\text{diag}(e^{-i\delta} \tanh \mathbf{r}) \end{array} \right] \left[\begin{array}{c|c} \mathbf{W} & \mathbf{0} \\ \hline \mathbf{0} & \mathbf{V}^T \end{array} \right]^T, \quad (\text{A11})$$

and the complex vector

$$\boldsymbol{\nu} = \begin{bmatrix} \alpha \\ \beta \end{bmatrix} \in \mathbb{C}^{2\ell}, \quad (\text{A12})$$

to finally write

$$\langle \alpha^* | \mathcal{D}(\gamma) \mathcal{U}(\mathbf{W}) \mathcal{S}(\zeta) \mathcal{U}(\mathbf{V}) | \beta \rangle = \exp \left(-\frac{1}{2} [||\alpha||^2 + ||\beta||^2] \right) C \exp \left(\boldsymbol{\mu}^T \boldsymbol{\nu} - \frac{1}{2} \boldsymbol{\nu}^T \Sigma \boldsymbol{\nu} \right), \quad (\text{A13})$$

where

$$C = \frac{\exp\left(-\frac{1}{2} [||\gamma||^2 + \gamma^\dagger \mathbf{W} \text{diag}(e^{i\delta} \tanh \mathbf{r}) \mathbf{W}^T \gamma^*]\right)}{\sqrt{\prod_{i=1}^\ell \cosh r_i}}, \quad (\text{A14})$$

$$\boldsymbol{\mu}^T = [\gamma^\dagger \mathbf{W} \text{diag}(e^{i\delta} \tanh \mathbf{r}) \mathbf{W}^T + \gamma^T, -\gamma^\dagger \mathbf{W} \text{diag}(\text{sech } \mathbf{r}) \mathbf{V}], \quad (\text{A15})$$

which is the expression quoted in the main text. Note that a related expression for the matrix elements of a general Gaussian transformations evaluated in the coordinate basis was worked out by Moshinsky and Quesne [33].

Appendix B: recurrence relation for the Taylor expansion coefficients of a Gaussian

We rewrite Eq. (15) of Ref. [40] in our notation as follows:

$$\Gamma_{\mathbf{k}+1_n} = \sum_{j=0}^{\mathbf{k}} \binom{\mathbf{k}}{j} Q^{(\mathbf{k}-j)} \Gamma_j, \quad (\text{B1})$$

where we write $\partial_{\mathbf{k}} f(\boldsymbol{\nu})|_{\boldsymbol{\nu}=0} = f^{(\mathbf{k})} = f_{\mathbf{k}}$ for the \mathbf{k}^{th} derivative of f at zero and define $\sum_{j=0}^{\mathbf{k}} \binom{\mathbf{k}}{j} = \sum_{j_1}^{k_1} \dots \sum_{j_n}^{k_n} \binom{k_1}{j_1} \dots \binom{k_n}{j_n}$. In our case Q is a quadratic in $\boldsymbol{\nu}$ and we write

$$Q(\boldsymbol{\nu}) = \boldsymbol{\mu}^T \boldsymbol{\nu} - \frac{1}{2} \boldsymbol{\nu}^T \boldsymbol{\Sigma} \boldsymbol{\nu}. \quad (\text{B2})$$

We can write easily all its nonzero derivatives:

$$Q^{(1_i)} = \mu_i, \quad (\text{B3})$$

$$Q^{(1_i+1_j)} = -\Sigma_{i,j}. \quad (\text{B4})$$

We know that most of the terms in Eq. (B1) will not survive the summation, indeed only the ones that satisfy $\mathbf{k} - \mathbf{j} = 1_i$ or $\mathbf{k} - \mathbf{j} = 1_i + 1_l$ will contribute to the sum. We can use this to our advantage and write

$$\Gamma_{\mathbf{k}+1_n} = Q^{(1_n)} \Gamma_{\mathbf{k}} + \sum_l k_l Q^{(1_n+1_l)} \Gamma_{\mathbf{k}-1_l} \quad (\text{B5})$$

$$= y_n \Gamma_{\mathbf{k}} - \sum_l k_l \Sigma_{l,n} \Gamma_{\mathbf{k}-1_l}. \quad (\text{B6})$$

Now let us derive this in a different way. Start with the generating function of the multidimensional Hermite polynomials [51–53]:

$$\exp\left(\boldsymbol{\mu}^T \boldsymbol{\nu} - \frac{1}{2} \boldsymbol{\nu}^T \boldsymbol{\Sigma} \boldsymbol{\nu}\right) = \sum_{\mathbf{k}=0}^{\infty} \frac{\boldsymbol{\nu}^{\mathbf{k}}}{\mathbf{k}!} G_{\mathbf{k}}^{(\boldsymbol{\Sigma})}(\boldsymbol{\mu}). \quad (\text{B7})$$

They satisfy the recurrence relation

$$G_{\mathbf{k}+1_i}^{(\boldsymbol{\Sigma})}(\boldsymbol{\mu}) = \mu_i G_{\mathbf{k}}^{(\boldsymbol{\Sigma})}(\boldsymbol{\mu}) - \sum_{j=1} \Sigma_{i,j} k_j G_{\mathbf{k}-1_j}^{(\boldsymbol{\Sigma})}(\boldsymbol{\mu}),$$

from which we identify that for a quadratic function Q ,

$$\Gamma_{\mathbf{k}} = G_{\mathbf{k}}^{(\boldsymbol{\Sigma})}(\boldsymbol{\mu}) = \sqrt{\mathbf{k}!} \mathcal{G}_{\mathbf{k}}. \quad (\text{B8})$$

By replacing this last expression in the recurrence relation Eq. (B5), and simplifying the factorials one arrives at the recurrence relation Eq. (28) for the matrix elements $\mathcal{G}_{\mathbf{k}}$.

Gate	Parameter $u = xe^{i\epsilon}$	Generator h	Value of s
$D(\gamma)$	γ	a_1^\dagger	1
$S(\zeta)$	$\zeta = re^{i\delta}$	$-\frac{1}{2} a_1^{\dagger 2}$	$\frac{1}{2}$
$S^{(2)}(\zeta)$	$\zeta = re^{i\delta}$	$a_1^\dagger a_2^\dagger$	1
$B(\theta, \varphi)$	$\theta e^{i\varphi}$	$a_1 a_2^\dagger$	-1

TABLE II. Parametrizations of different common Gaussian gates and their s -parameter necessary to obtain the gradient with respect to their phase.

Appendix C: Gradients of a single complex-parameter gate

We outline here an alternative procedure to obtain gradients of single-parameter gates. Let us consider a gate parametrized by a single complex number $u = xe^{i\epsilon}$,

$$G(u) = G(xe^{i\epsilon}) = \exp(xe^{i\epsilon} h - \text{H.c.}). \quad (\text{C1})$$

For example, for a two-mode squeezing gate, $h = a_1^\dagger a_2^\dagger$. Now it is direct to verify that

$$\partial_x \langle \mathbf{m} | G | \mathbf{n} \rangle = \langle \mathbf{m} | G \{ e^{i\epsilon} h - \text{H.c.} \} | \mathbf{n} \rangle. \quad (\text{C2})$$

To obtain the gradient with respect to the amplitude x , one only needs to express $h|\mathbf{n}\rangle$ and $h^\dagger|\mathbf{n}\rangle$ in terms of a linear combination of Fock states to reduce the gradient to a linear combination of the matrix elements of the gate itself. Again using the two-mode squeezing gate as an example we easily find

$$\partial_x \langle \mathbf{m} | G | \mathbf{n} \rangle = \langle m_1, m_2 | G \{ a_1^\dagger a_2^\dagger e^{i\epsilon} - \text{H.c.} \} | n_1, n_2 \rangle \quad (\text{C3})$$

$$= \sqrt{(n_1+1)(n_2+1)} e^{i\epsilon} G_{m_1, m_2, n_1+1, n_2+1} - \sqrt{n_1 n_2} e^{-i\epsilon} G_{m_1, m_2, n_1-1, n_2-1}. \quad (\text{C4})$$

Let us consider the gradient with respect to the phase: one would hope that a formula similar to Eq. (C2) should hold. Unfortunately this is not the case, the reason being that two gates with the same phase parameter commute with each other, $[G(xe^{i\epsilon}), G(x'e^{i\epsilon})] = 0$ but the same commutativity does not hold for different values of the phase, $[G(xe^{i\epsilon}), G(xe^{i\epsilon'})] \neq 0$. To make progress we note that for any of the single complex-parameter gates one

can obtain the following simple decomposition:

$$G(xe^{i\epsilon}) = R_1(s\epsilon)G(x)R_1^\dagger(s\epsilon), \quad (\text{C5})$$

where $R_1(s\epsilon) = e^{is\epsilon a_1^\dagger a_1}$ is a rotation gate. We summarize the values of the different parameters in this decomposition in Table II for the single- and two-mode gate studied in the main text. With this decomposition we can now take derivatives of matrix elements with respect to the phase argument of the complex parameter,

$$\partial_\epsilon \langle \mathbf{m} | G | \mathbf{n} \rangle = \langle \mathbf{m} | (\partial_\epsilon R_1(s\epsilon)) G(x) R_1^\dagger(s\epsilon) \quad (\text{C6})$$

$$+ R_1(s\epsilon) G(x) (\partial_{s\epsilon} R_1^\dagger(s\epsilon)) | \mathbf{n} \rangle$$

$$= \langle \mathbf{m} | (i s a_1^\dagger a_1) R_1(s\epsilon) G(x) R_1^\dagger(s\epsilon) \quad (\text{C7})$$

$$+ R_1(s\epsilon) G(x) R_1^\dagger(s\epsilon) (-i s a_1^\dagger a_1) | \mathbf{n} \rangle$$

$$= i s (m_1 - n_1) \langle \mathbf{m} | G | \mathbf{n} \rangle. \quad (\text{C8})$$

-
- [1] M. Schuld, V. Bergholm, C. Gogolin, J. Izaac, and N. Killoran, Phys. Rev. A **99**, 032331 (2019).
- [2] M. Benedetti, E. Lloyd, S. Sack, and M. Fiorentini, Quantum Sci. Technol. **4**, 043001 (2019).
- [3] V. Dunjko, J. M. Taylor, and H. J. Briegel, Phys. Rev. Lett. **117**, 130501 (2016).
- [4] I. Kerenidis, J. Landman, A. Luongo, and A. Prakash, in *Advances in Neural Information Processing Systems* (2019) pp. 4136–4146.
- [5] J. M. Arrazola, T. R. Bromley, J. Izaac, C. R. Myers, K. Brádler, and N. Killoran, Quantum Sci. Technol. **4**, 024004 (2019).
- [6] N. Killoran, T. R. Bromley, J. M. Arrazola, M. Schuld, N. Quesada, and S. Lloyd, Phys. Rev. Res. **1**, 033063 (2019).
- [7] N. Killoran, J. Izaac, N. Quesada, V. Bergholm, M. Amy, and C. Weedbrook, Quantum **3**, 129 (2019).
- [8] G. R. Steinbrecher, J. P. Olson, D. Englund, and J. Carolan, npj Quantum Inf. **5**, 1 (2019).
- [9] N. Quesada, L. Helt, J. Izaac, J. Arrazola, R. Shahrokhshahi, C. Myers, and K. Sabapathy, Phys. Rev. A **100**, 022341 (2019).
- [10] J. Romero, J. P. Olson, and A. Aspuru-Guzik, Quantum Sci. Technol. **2**, 045001 (2017).
- [11] M. Schuld, A. Bocharov, K. M. Svore, and N. Wiebe, Phys. Rev. A **101**, 032308 (2020).
- [12] M. Schuld and N. Killoran, Phys. Rev. Lett. **122**, 040504 (2019).
- [13] V. Havlíček, A. D. Córcoles, K. Temme, A. W. Harrow, A. Kandala, J. M. Chow, and J. M. Gambetta, Nature **567**, 209 (2019).
- [14] P. J. O'Malley, R. Babbush, I. D. Kivlichan, J. Romero, J. R. McClean, R. Barends, J. Kelly, P. Roushan, A. Tranter, N. Ding, *et al.*, Phys. Rev. X **6**, 031007 (2016).
- [15] A. Peruzzo, J. McClean, P. Shadbolt, M.-H. Yung, X.-Q. Zhou, P. J. Love, A. Aspuru-Guzik, and J. L. O'Brien, Nature Commun. **5**, 4213 (2014).
- [16] A. Politi, J. C. Matthews, M. G. Thompson, and J. L. O'Brien, IEEE J. Sel. Top. Quantum Electron. **15**, 1673 (2009).
- [17] Y. Zhang, M. Menotti, K. Tan, V. Vaidya, D. Mahler, L. Zatti, M. Liscidini, B. Morrison, and Z. Vernon, arXiv preprint arXiv:2001.09474 (2020).
- [18] V. Vaidya, B. Morrison, L. Helt, R. Shahrokhshahi, D. Mahler, M. Collins, K. Tan, J. Lavoie, A. Repington, M. Menotti, *et al.*, arXiv preprint arXiv:1904.07833 (2019).
- [19] S. Lloyd and S. L. Braunstein, in *Quantum information with continuous variables* (Springer, 1999) pp. 9–17.
- [20] A. Serafini, *Quantum continuous variables: a primer of theoretical methods* (CRC Press, 2017).
- [21] C. Weedbrook, S. Pirandola, R. García-Patrón, N. J. Cerf, T. C. Ralph, J. H. Shapiro, and S. Lloyd, Rev. Mod. Phys. **84**, 621 (2012).
- [22] S. Barnett and P. M. Radmore, *Methods in theoretical quantum optics*, Vol. 15 (Oxford University Press, 2002).
- [23] K. E. Cahill and R. J. Glauber, Phys. Rev. **177**, 1857 (1969).
- [24] P. Král, J. Mod. Opt. **37**, 889 (1990).
- [25] N. Quesada, *Very Nonlinear Quantum Optics*, Ph.D. thesis, University of Toronto (2015).
- [26] I. Dhand, B. C. Sanders, and H. de Guise, J. Math. Phys. **56**, 111705 (2015).
- [27] E. Doktorov, I. Malkin, and V. Man'ko, J. Mol. Spectrosc. **64**, 302 (1977).
- [28] D. Gruner and P. Brumer, Chem. Phys. Lett. **138**, 310 (1987).
- [29] R. Berger, C. Fischer, and M. Klessinger, J. Phys. Chem. A **102**, 7157 (1998).
- [30] V. Mozhayskiy, S. Gozem, and A. I. Krylov, “ezspectrum v3.0,” <http://iopenshell.usc.edu/downloads/> (2016).
- [31] J. Huh, *Unified description of vibronic transitions with coherent states*, Ph.D. thesis, Johann Wolfgang Goethe-Universität in Frankfurt am Main (2011).
- [32] S. M. Rabidoux, V. Eijkhout, and J. F. Stanton, J. Chem. Theory Comput. **12**, 728 (2016).
- [33] M. Moshinsky and C. Quesne, J. Math. Phys. **12**, 1772

- (1971).
- [34] K. B. Wolf, J. Math. Phys. **15**, 1295 (1974).
 - [35] P. Kramer, M. Moshinsky, and T. Seligman, in *Group Theory and Its Applications*, edited by E. Loebl (Academic, New York, 1975) pp. 250–300.
 - [36] B. Gupt, J. Izaac, and N. Quesada, J. Open Source Softw. **4**, 1705 (2019).
 - [37] A. Björklund, B. Gupt, and N. Quesada, ACM J. Exp. Algorithmics **24**, 11 (2019).
 - [38] N. Quesada, J. Chem. Phys. **150**, 164113 (2019).
 - [39] C. Bloch and A. Messiah, Nucl. Phys. **39**, 95 (1962).
 - [40] F. M. Miatto, arXiv preprint arXiv:1911.11722 (2019).
 - [41] G. Cariolaro and G. Pierobon, Phys. Rev. A **94**, 062109 (2016).
 - [42] A. B. Klimov and S. M. Chumakov, *A group-theoretical approach to quantum optics: models of atom-field interactions* (John Wiley & Sons, 2009).
 - [43] R. Hunger, *An introduction to complex differentials and complex differentiability*, Tech. Rep. (2007).
 - [44] D. Gottesman, A. Kitaev, and J. Preskill, Phys. Rev. A **64**, 012310 (2001).
 - [45] J. Huh, arXiv preprint arXiv:2004.05766 (2020).
 - [46] S. v. d. Walt, S. C. Colbert, and G. Varoquaux, Comput. Sci. Eng. **13**, 22 (2011).
 - [47] P. Virtanen, R. Gommers, T. E. Oliphant, M. Haberland, T. Reddy, D. Cournapeau, E. Burovski, P. Peterson, W. Weckesser, J. Bright, S. J. van der Walt, M. Brett, J. Wilson, K. Jarrod Millman, N. Mayorov, A. R. J. Nelson, E. Jones, R. Kern, E. Larson, C. Carey, Í. Polat, Y. Feng, E. W. Moore, J. VanderPlas, D. Laxalde, J. Perktold, R. Cimrman, I. Henriksen, E. A. Quintero, C. R. Harris, A. M. Archibald, A. H. Ribeiro, F. Pedregosa, P. van Mulbregt, and SciPy 1.0 Contributors, Nat. Methods **17**, 261 (2020).
 - [48] T. Kluyver, B. Ragan-Kelley, F. Pérez, B. E. Granger, M. Bussonnier, J. Frederic, K. Kelley, J. B. Hamrick, J. Grout, S. Corlay, *et al.*, in *ELPUB* (2016) pp. 87–90.
 - [49] J. D. Hunter, Comput. Sci. Eng. **9**, 90 (2007).
 - [50] S. K. Lam, A. Pitrou, and S. Seibert, in *Proceedings of the Second Workshop on the LLVM Compiler Infrastructure in HPC* (2015) pp. 1–6.
 - [51] S. Berkowitz and F. Garner, Math. Comput. **24**, 537 (1970).
 - [52] P. Kok and S. L. Braunstein, J. Phys. A: Math. Gen. **34**, 6185 (2001).
 - [53] M. M. Mizrahi, J. Comput. Appl. Math. **1**, 137 (1975).